Int J Adv Manuf Technol (2017) 93:617–622
DOI 10.1007/s00170-017-0548-y

ORIGINAL ARTICLE

Drop and tilt method of five-axis tool positioning for tensor product surfaces

Ravinder Kumar Duvedi[1] · Sanjeev Bedi[2] · Stephen Mann[2]

Received: 7 March 2017 / Accepted: 9 May 2017 / Published online: 23 May 2017

Abstract The drop and tilt tool positioning method for five-axis machining with a toroidal tool positions the toroidal tool to have two points of contact with a triangulated surface. In this paper, we extend the method to position the tool with two points of contact on algebraically defined tensor product Bézier surfaces.

Keywords CNC machining · Five-axis machining · Multipoint machining

1 Introduction

Research on machining of curved surfaces for dies and molds has been pursued by many researchers and research labs. The challenges in five-axis machining of these curved surfaces are machining time and surface finish. Industry wants smaller machining times and better surface finishes. Known methods for five-axis machining of curved surfaces fall broadly in two main categories. In the first category, the tool is positioned so that at the point of contact with the design surface, the shape of the tool matches the shape of the surface. Such matching is achieved by equating curvature or some simple measure of it [1, 10, 11]. In the second broad category, the tool is positioned so that the tool touches the design surface at multiple points simultaneously [3–5, 7, 12–14]; the contact at one point is easy to obtain, but methods of finding the second point vary. In both categories, the tool travels close to the designed surface. The deviation between the design surface and the surface swept by the moving tool is small and can be controlled. When the deviation is well within the tolerance specified by the user, a single machining pass made of connected consecutive five-axis tool positions can machine a strip that does not require polishing, etc. If the entire surface can be machined with such passes, then the number of passes required to machine the entire surface is few. With fewer passes required to machine the surface, the machining time is reduced [8, 9, 15]. Both categories of five-axis machining methods use a radiused (toroidal) end mill. The cutting characteristics of a radiused end mill are better at the bottom tip of tool [2] and along the sides in comparison to ball end and flat end mill. Further, the radiused end mill is a generalization of both ball end mill and flat end mill [3, 5]. Any method developed for the toroidal end mill can in limiting cases be applied to flat and ball end mills as well.

In this work, a method for positioning the tool of a five-axis machine onto a triangulated surface [3] is extended to tensor product Bézier surfaces. Since tensor product B-splines can be simplified into a patch work of tensor product Bézier surfaces, the method can be applied to them as well, although some issues still remain to handle patch boundaries. We tested our algorithm on bi-quadric tensor product Bézier surfaces, and the algorithm successfully computed toolpaths for these surfaces, one of which we used to machine a part.

In Section 3, we describe how to drop the tool to find a first point of contact and then tilt the tool onto a tensor product Bézier surface to find a second point of contact.

✉ Stephen Mann
smann@uwaterloo.ca

Ravinder Kumar Duvedi
rduvedi@gmail.com

Sanjeev Bedi
sbedi@uwaterloo.ca

[1] Thapar University, Patiala, Punjab, India

[2] University of Waterloo, Waterloo, ON, Canada

Machining tests are given in Section 4, with a discussion of the method, and its weaknesses appearing in Section 5.

2 Background

Mathematically defined parametric surfaces for representing the sculptured surfaces include Bézier, B-spline, and NURBS (non-rational B-spline surfaces). Bézier surfaces are one of the simplest form of parametric surface representation and B-splines can be converted to the Bézier representation. In this work, we study the development of five-axis tool positioning for toroidal end mill cutters for multipoint machining of Bézier surfaces. The generalized radiused end mill cutter can be defined by the radius of the minor circle R_i representing circular inserts or *pseudo-inserts* and the radius of major circle of torus R_o, as shown in Fig. 1. The multipoint five-axis tool positioning with a radiused end mill cutter ensures that the finish surface machining can be achieved with a fewer number of machining passes [4]; although the width of the cut is larger than single point five-axis machining, the forces generated are within the scope of the maximum five-axis machining centers [12]. This is a benefit for the manufacturing industry as multipoint machining can yield significant time savings.

Different approaches have been developed over the last two decades for multipoint five-axis tool positioning, but these methods use approximate or numerical methods to arrive at the solution. Methods like the principle axis method [10, 15], the principle curvature alignment technique [1], the rolling ball method [6], multipoint machining method [13, 14], and the recently developed drop and tilt method (DTM) [3, 4] use special techniques to arrive at the best possible inclination of toroidal cutter while ensuring the multipoint tangency of cutting tool with the machined surface. However, the approximations used for the numerical solution may not yield the optimum solution under varying surface curvatures. In this work, we extend DTM from triangulated surfaces to tensor product Bézier patches.

DTM [3] separates the positioning process into two steps. In the first step, the tool is dropped vertically on the triangulated surface to identify the highest point of contact on the machined surface, while in the second step, a bi-section approach is used to identify the maximum possible tilt of tool axis. The tool is tilted about the center of pseudo-insert at first point of contact in such a way that it retains its tangency at the first point of contact while searching for a second point of tangency. Though the DTM approach for triangulated surfaces is computationally efficient, the errors arising because of triangulation of a parametric surface were ignored. If higher accuracy triangulated meshes are used, then the triangulated data itself becomes large and increases the overall computation time.

In this work, we have developed a direct mathematical model for multipoint five-axis tool positioning of a toroidal milling cutter for machining of a bi-quadratic Bézier surface. The developed approach is an extension of the drop and tilt method for triangulated surfaces.

As the focus of this work was positioning a toroidal tool with two points of contact, we used the zig-zag machining pass as shown in Fig. 2; this trajectory is called the *tool path footprint*.

We used a bi-quadratic tensor product Bézier surface as surface model; its representation is

$$S(u,v) = \sum_{i=0}^{2}\sum_{j=0}^{2} P_{i,j} B_i^2(u) B_j^2(v),$$

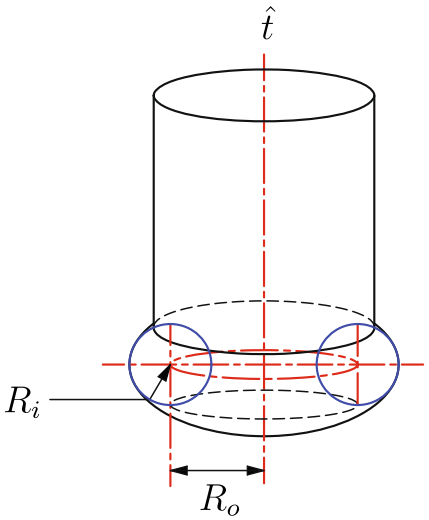

Fig. 1 The geometric model of the radiused endmill used in this work

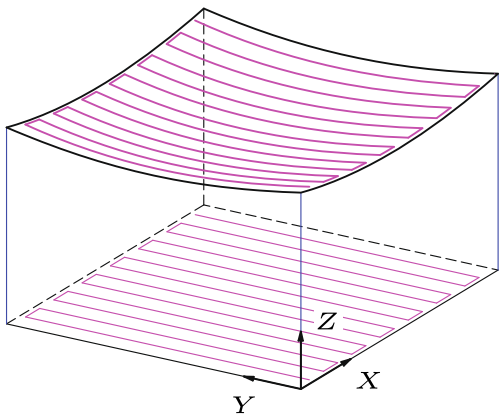

Fig. 2 Toolpath footprint used for locating the first point of contact zig-zag toolpath

with $0 \leq u$ and $v \leq 1$ and where the $P_{i,j}$ are control points used to define the surface and

$$B_i^n(u) = \binom{n}{i} u^i (1-u)^{n-i}.$$

3 Proposed method

Starting with a point T on the tool footprint, we drop the tool along the tool axis $\hat{t}$ and find a first point of contact P on the surface S at $S(u_1, v_1)$; we denote the normal to S at P as $\hat{n}_P$. The pseudo-insert on the tool through P has center O_1 (Fig. 3a). We construct a coordinate frame $\hat{i}, \hat{j}, \hat{k}$ at P with $\hat{i}$ perpendicular to the plane of the pseudo-insert, $\hat{k} = \hat{t}$, and $\hat{j} = \hat{k} \times \hat{i}$.

As we rotate the tool around $\hat{i}$ (so that the tool remains tangent to S at P), we construct a new local coordinate system $\hat{i}_1, \hat{j}_1, \hat{k}_1$ with $\hat{i}_1 = \hat{i}$ (Fig. 3b). As we rotate the tool around $\hat{i}$, the tool will eventually contact S at a second point of contact, $Q = S(u_2, v_2)$. The following two subsections give the mathematical details of these operations.

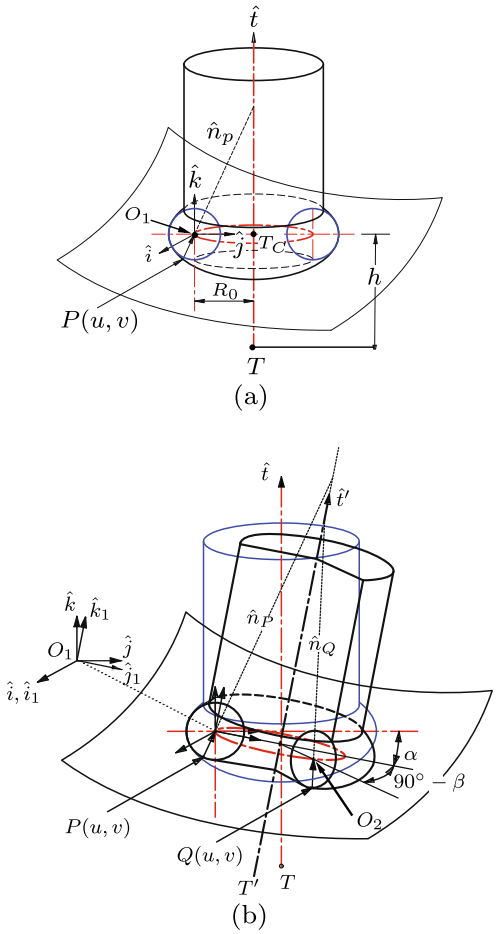

Fig. 3 **a** Drop the tool. **b** Tilt the tool

3.1 Stage 1: drop the tool

The toroidal tool with radius of insert R_i and offset radius R_o is dropped along a predetermined tool-axis direction $\hat{t}$ at the tool footprint location T on the bi-quadric Bézier surface $S(u, v)$. A point on the surface of the toroidal tool centered at T_C can be represented as

$$P = T_C - \hat{n}_P R_i - \hat{j} R_o,$$

where $\hat{n}_P$ is the normal to the torus at P and $\hat{j}$ is a unit vector perpendicular to the tool axis. The motion of the dropping tool center T_C is given by

$$T_C(h) = T + h\hat{t}.$$

Let the first point of contact between the tool and the Bézier surface be $P = S(u_1, v_1)$, where the tool and the surface touch tangentially. Then, P can be determined using the following relationship:

$$S(u,v) - P = S(u,v) + \hat{n}(u,v) R_i + \hat{j} R_o - T - \hat{t} h = 0 \quad (1)$$

where

$$\begin{aligned} \hat{k} &= \hat{t} \\ \hat{i} &= (\hat{n}(u,v) \times \hat{k}) / \|\hat{n}(u,v) \times \hat{k}\| \\ \hat{j} &= (\hat{k} \times \hat{i}) / |\hat{k} \times \hat{i}\| \\ \hat{n}(u,v) &= \frac{\frac{\partial S}{\partial u} \times \frac{\partial S}{\partial v}}{\|\frac{\partial S}{\partial u} \times \frac{\partial S}{\partial v}\|}. \end{aligned} \quad (2)$$

Note that in Eq. 1, we have replaced the normal to the toroidal tool with the normal to the surface S, a necessary condition for the two to meet tangentially.

The above equations can be solved to determine the values of parameters $u = u_1$, $v = v_1$, and h; since there are multiple solutions, we choose the one with the highest value of h. We can then find the location of the first point of contact $P = S(u_1, v_1)$ for the dropping tool as well as the orientation of the surface normal at the first point of contact given by $\hat{n}_P = \hat{n}(u_1, v_1)$.

3.2 Stage 2: finding the angle of inclination of the tool-axis and the second point of contact

In the second stage, the tool is rotated about the pseudo-insert axis $\hat{i}$ through the center of the pseudo-insert O_1 at the first point of contact P. The location of center of the pseudo-insert O_1 is given as

$$O_1 = P + \hat{n}_P R_i.$$

The coordinate frame defined by direction vectors $(\hat{i}, \hat{j}, \hat{k})$ is established at center of the pseudo-insert. The axis of the toroidal cutter $\hat{t}$ is rotated by an angle α about $\hat{i}$ to a new orientation $\hat{t}' = \hat{k}_1$. In this case, the tool touches S at a

```
DropAndTilt(S, Tool, T)
    1. Drop Tool along t̂ through T onto S
        1.1 Solve (1) for u1, v1, h
        1.2 Compute P = S(u1, v1)
        1.3 Compute î, ĵ, k̂, n̂P from (2)
        1.4 Compute O1 = P + n̂P(u1, v1)Ri
    2. Tilt Tool around O1 about î
        2.1 Solve (5) and (6) for u2, v2, α, β
        2.2 Compute t̂′ = −ĵ sin(α) + k̂ cos(α)
    Return P, n̂P(u1, v1), t̂′
```

Fig. 4 Pseudo-code of drop and tilt algorithm for dropping a tool onto the tensor product Bézier surface $S(u, v)$ from a point T on the toolpath

second point of contact $Q = S(u_2, v_2)$. To find Q, we note that after rotating by α around $\hat{i}$, the tool center T_C is located at

$$T_C = O_1 + \hat{j}_1 R_o \tag{3}$$

and that Q is located at

$$Q = T_C + (\hat{i}_1 \cos(\beta) + \hat{j}_1 \sin(\beta))R_o - \hat{n}_Q R_i, \tag{4}$$

where $\hat{n}_Q$ is the normal to the torus at Q. Combining Eqs. 3 and 4 to eliminate T_C, equating to $S(u, v)$, and requiring $\hat{n}_Q = \hat{n}(u, v)$ yields the following simultaneous equation:

$$S(u, v) + \hat{n}(u, v)R_i - \left\{O_1 + R_o(\hat{j}_1 + \hat{i}_1 \cos(\beta) + \hat{j}_1 \sin(\beta))\right\} = 0. \tag{5}$$

where β is the rotation angle around $\hat{k}_1$ and where

$$\begin{aligned} \hat{i}_1 &= \hat{i} \\ \hat{j}_1 &= \hat{j}\cos(\alpha) + \hat{k}\sin(\alpha), \\ \hat{k}_1 &= \hat{t}' = -\hat{j}\sin(\alpha) + \hat{k}\cos(\alpha). \end{aligned}$$

Equation 5 has four unknowns, namely u, v, α, and β, but expands to only three coordinate equations. As a fourth constraint on the unknowns, we ensure that the shortest distance from the tool axis to the normal to the surface at the second point of contact is zero:

$$\{(O_1 + R_o\hat{j}_1) - S(u, v)\} \cdot \{\hat{t}' \times \hat{n}(u, v)\} = 0, \tag{6}$$

where $\hat{t}'$ is the rotated tool axis.

Figure 4 gives pseudo-code for our implementation of the drop and tilt method. This routine is called for each point on the tool footprint. In steps 1.1 and 2.1, the equations were solved using the symbolic algebra environment Maple™.

4 Example

The method was successfully tested on concave, flat, and convex surfaces. Here, we give the example of the DTM positioning the tool on a concave bi-quadric Bézier surface shape. The control points used for the Bézier surface patch are shown in Table 1; the surface itself appears in Fig. 5. These control points have been chosen to lie in the bounds of a square of 150 mm × 150 mm. The five-axis multipoint tool path data was generated for 13 machining passes having a side step of 12.5 mm. In each machining pass, a feed forward step of 2.5 mm was maintained between two adjacent tool positions. The zig-zag machining pass selected in the present study is as shown in Fig. 2.

Using code for the DTM developed in Maple™, we generated multipoint five-axis tool position data for each tool footprint locations for all zig-zag machining passes. The accuracy of the developed five-axis toolpath data is verified using a custom 3D graphical simulator developed in using graphics in the Maple™ symbolic algebra environment. Figure 6 shows the 3D graphical simulation plot from Maple™ graphics where every tenth tool position for each machining pass is shown; both a view from above the surface and a view from below the surface are shown in the figure. The circular mark in the bottom view of Fig. 6a represents the contact between the Bézier surface and the bottom of the toroidal cutter; although there are only two points of contact, a circle of the torus shows through the bottom of the Bézier surface due to the way Maple™ renders surfaces that are close to one another.

In addition to graphical verification of the five-axis toolpath data, we also tested it by machining an aluminum specimen on a DMU-80P Hi-Dyn tilt-rotary simultaneous five-axis machining center. The five-axis machining resulted in the anticipated smooth machined part surface which is shown in Fig. 7. The cutter motion from one tool location to the next was in an almost linear passion. The few visible marks on the smooth machined surface are the results of shift in the tool inclination while it moved from one side of convex Bézier surface towards another side in a machining pass.

5 Discussion

The drop and tilt method of five-axis tool positioning for parametric surface is a two step procedure. In the first step,

Table 1 Control points for test surface

$P_{0,0} = (0.0, 0.0, 89.1)$	$P_{0,1} = (75.0, 0.0, 74.25)$	$P_{0,2} = (150.0, 0.0, 89.1)$
$P_{1,0} = (0.0, 75.0, 79.2)$	$P_{1,1} = (75.0, 75.0, 74.25)$	$P_{1,2} = (150.0, 75.0, 69.3)$
$P_{2,0} = (0.0, 150.0, 89.1)$	$P_{2,1} = (75.0, 150.0, 74.25)$	$P_{2,2} = (150.0, 150.0, 84.15)$

Fig. 5 Bi-quadric test surface

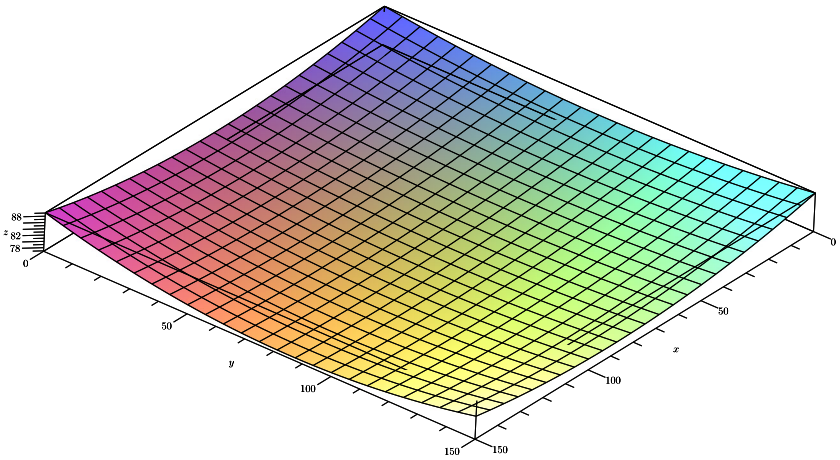

the first point of tangency of the toroidal cutter and the machined surface at the predetermined tool-axis orientation for a given toolpath footprint location is determined. The second step determines a second point of tangency of toroidal cutter and the machined surface at a tilted tool-axis orientation. This procedure is independent of the toolpath footprint pattern used. The two steps used to determine the first and second point of contact in the DTM algorithm for a Bézier surface are sequential, with which the location of first point of contact $P(u, v)$ and surface normal at first point of contact $\hat{n}_P(u, v)$ are used in the solver to determine the parameters required to find the second point of contact. During the drop stage, the shank of the tool does not impact the tool positioning approach as it is hidden behind the toroidal cutting edge of the tool facing towards the machined surface; during rotation, the shank may potentially impact the tool positioning, but we did not consider this in our proof of concept implementation.

The simulation results demonstrated the gouge-free multipoint tangency of the cutting end of the toroidal end mill on the Bézier surface patch in the form of circular rings representing bottom of the toroidal cutter as apparent from the bottom view of simulator results shown in Fig. 6a. The same five-axis toolpath data was further used for machining of the Bézier surface on a DMU 80-P Hi-Dyn tilt-rotary simultaneous five-axis machining center. The five-axis machined surface demonstrated consistency with the simulation results as shown in Fig. 7.

Overall, the present work opens a venue for computation of multipoint five-axis tool positioning data directly from a parametric Bézier patch. This approach is able

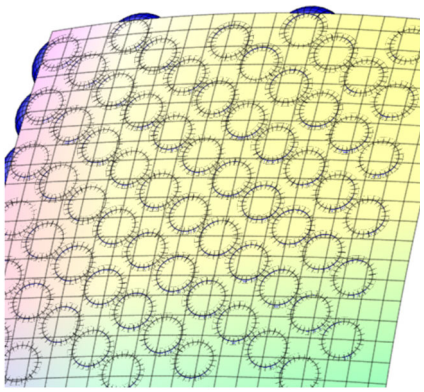

(a)

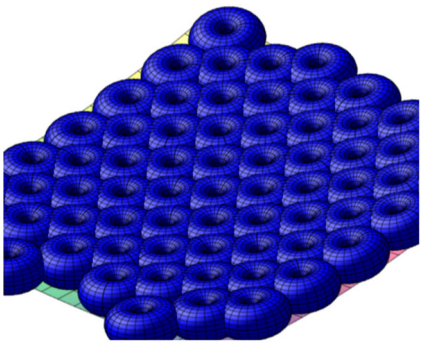

(b)

Fig. 6 **a** Bottom view and **b** top view of simulated tool path

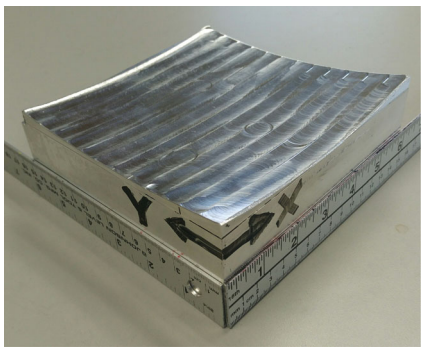

Fig. 7 Machined part

to yield accurate tool positioning data and can help to eliminate the need for approximation of the parametric part surface using triangulated patches as reported in our earlier work on the evolution of the DTM for triangulated surface models [11, 12, 14]. However, significant development remains to make the method usable in an industrial setting. In particular, a numerical method is needed for solving the equations; in addition to performance issues, such a method should allow an extension from bi-quadratic patches to higher degree surfaces and NURBS.

Furthermore, industrial surfaces are composed of multiple parametric surface patches that may have different types of surface continuities among the constituent patches. Two surface patches may have a common raised sharp edge or a group of constituent patches may have a common raised corner. While machining an independent surface patch, the toroidal cutter has to move over patch boundaries. Further investigation is required to handle multipoint tool positioning solutions when the cutter traverses over common edges and corners between parametric Bézier patches.

6 Conclusion

The work described in this paper presented a unique approach for multipoint five-axis tool positioning of a toroidal milling cutter directly over a bi-quadratic Bézier surface patch. The work presented in this paper is a proof of the concept for direct implementation of the drop and tilt method for Bézier surfaces. It opens the door for development of a method for multipoint machining of Bézier surfaces in a commercial package. However, additional work is required to evolve the developments of this work into a numerical implementation that can be used for industrial applications. Further, investigation of issues such as undercut and finding the optimal toolpath for maximum strip width remains to be done.

References

1. Bedi S, Gravelle S, Chen Y (1997) Principal curvature alignment technique for machining complex surfaces. J Manuf Sci Eng 119(4B):756–765
2. Bedi S, Ismail F, Mahjoob MJ, Chen Y (1997) Toroidal versus ball nose and flat bottom end mills. Int J Adv Manuf 13(5):326–332
3. Duvedi RK, Bedi S, Batish A, Mann S (2014) A multipoint method for 5-axis machining of triangulated surface models. Comput Aided Des 52:17–26
4. Duvedi RK, Bedi S, Batish A, Mann S (2015) Numeric implementation of drop and tilt method of 5-axis tool positioning for machining of STL surfaces. Int J Adv Manuf Technol 78(9–12):1677–1690
5. Duvedi RK, Bedi S, Batish A, Mann S (2016) The edge–torus tangency problem in multipoint machining of triangulated surface models. Int J Adv Manuf Technol 82(9):1959–1972
6. Gray P, Ismail F, Bedi S (2005) Graphics-assisted rolling ball method for 5-axis surface machining. Comput-Aided Des 36(7):653–663
7. He Y, Chen Z (2014) Optimising tool positioning for achieving multi-point contact based on symmetrical error distribution curve in sculptured surface machining. Int J Adv Manuf Technol 73(4):707–714
8. Lasemi A, Xue D, Gu P (2010) Recent development in CNC machining of freeform surfaces: a state-of-the-art review. Comput-Aided Des 42:641–654
9. Patel K, Bolanos GS, Bassi R, Bedi S (2011) Optimal tool shape selection based on surface geometry for three-axis CNC machining. Int J Adv Manuf Technol 57:655–670
10. Rao N, Bedi S, Buchal R (1996) Implementation of the principal-axis method for machining of complex surfaces. Int J Adv Manuf Technol 11(4):249–257
11. Rao N, Ismail F, Bedi S (1997) Tool path planning for five-axis machining using the principal axis method. Int J Mach Tools Manuf 37(7):1025–1040
12. Roth D, Ismail F, Bedi S (2005) Mechanistic modelling of the milling process using complex tool geometry. Int J Adv Manuf Technol 25:140–144
13. Warkentin A, Ismail F, Bedi S (2000) Comparison between multi-point and other 5-axis tool positioning strategies. Int J Mach Tools Manuf 40(2):185–208
14. Warkentin A, Ismail F, Bedi S (2000) Multi-point tool positioning strategy for 5-axis machining of sculptured surfaces. Comput Aided Geom Des 17(1):83–100
15. Yaua HT, Chuanga CM, Lee YS (2004) Numerical control machining of triangulated sculptured surfaces in a stereo lithography format with a generalized cutter. Int J Protein Res 42(13):2573–2598